Applied Thermal Engineering 208 (2022) 117991

Contents lists available at ScienceDirect

Applied Thermal Engineering

journal homepage: www.elsevier.com/locate/apthermeng

Parametric investigation and optimal selection of the hybrid turbocharger system for a large marine four-stroke dual-fuel engine

Massimo Figari [a,*], Gerasimos Theotokatos [b], Andrea Coraddu [c], Sokratis Stoumpos [b], Teresa Mondella [a]

[a] DITEN – University of Genova, Via Opera Pia 11a, I-16145 Genova, Italy
[b] Maritime Safety Research Centre, Department of Naval Architecture, Ocean & Marine Engineering, University of Strathclyde, 100 Montrose Street, Glasgow G4 0LZ, UK
[c] Faculty of Mechanical, Maritime and Materials Engineering, Delft University of Technology, Mekelweg 5, 2628 CD Delft, Netherlands

ARTICLE INFO

Keywords:
Hybrid turbocharger
Marine Dual fuel engine
Simulation
Impact quantification
Actual operating profile
Optimal size selection

ABSTRACT

Hybrid turbochargers can become an attractive solution for new built and retrofitted ship power plants, as their use can result in increasing the plant efficiency and reducing emissions. This study aims at computationally investigating the hybrid turbocharger effects on a large marine dual-fuel four-stroke engine performance and emissions characteristics as well as determining its electrical generator optimal size for the case of a ship power plant considering an actual operating profile. An existing model of a large marine four-stroke dual-fuel engine of the zero/one-dimensional type, which was developed in the commercial software GT-Power, is extended to include the hybrid turbocharger sub-model. This model is subsequently employed to carry out a parametric investigation considering a wide range for the hybrid turbocharger electric motor power. The derived results are analysed to identify the variations of the investigated dual fuel engine performance and emissions parameters in the whole engine operating envelope at both the diesel and gas modes, whilst taking into account the engine and its components operational limits. For the considered annual load profile, the results demonstrate that the optimal nominal size of the hybrid turbocharger electric motor power is 300 kW and leads to an annual energy surplus between 2% and 3% of the annually delivered engine mechanical energy. This study benefits the quantification of the hybrid turbocharger impact on large marine dual fuel four-stroke engines as well as the ship energy efficiency, thus providing useful decision support to facilitate the shipboard implementation of this technology.

1. Introduction

The shipping industry has been facing an immense pressure to render its operations more sustainable and reduce its environmental footprint. Responding to the international and national regulatory frameworks for reducing carbon emissions as well as considering the short-term and long-term policies for reducing the greenhouse effects, initiatives towards designing and building zero-emissions vessels need to be pursued. For addressing these challenges,

a combination of both design and operational measures/technologies are expected to be adopted in new built and existing ships. Operational measures include slow steaming as well as voyage and logistics planning [1–3]. Design measures include waste heat recovery [4], carbon capture, after- treatment systems, as well as alternative fuels and dual fuel (DF) engines. The use of Natural Gas as a marine fuel and dual-fuel engines is an effective way to comply with future carbon emissions requirements [5] as well as the challenges associated with the NO_x and SO_x emissions compliance [6].

A detailed analysis of several operational and design measures, along with the expected fuels savings and the carbon footprint, is reported in [7]; the CO_2 emissions reduction was estimated in the range of 15–25%

Abbreviations: CFD, Computational Fluid Dynamics; DE, Diesel Engine; DF, Dual Fuel; EEDI, Energy Efficiency Design Index; EM, Electric Machine; EGR, Exhaust Gas Re-circulation; EWG, Exhaust Waste Gate Valve; HFO, Heavy Fuel Oil; HRR, Heat Release Rate; HTC, Hybrid Turbocharger; IGBT, Insulated Gate Bipolar Transistor; IMO, International Maritime Organisation; KPI, Key Performance Indicator; LNG, Liquefied Natural Gas; MCR, Maximum Continuous Rating; MDO, Marine Diesel Oil; PI, Proportional Integral control; TC, Turbocharger.

* Corresponding author.
E-mail addresses: massimo.figari@unige.it (M. Figari), gerasimos.theotokatos@strath.ac.uk (G. Theotokatos), a.coraddu@tudelft.nl (A. Coraddu), sokratis.stoumpos@strath.ac.uk (S. Stoumpos), teresamondella@hotmail.it (T. Mondella).

https://doi.org/10.1016/j.applthermaleng.2021.117991
Received 4 September 2020; Received in revised form 28 November 2021; Accepted 20 December 2021
Available online 2 February 2022

Nomenclature

$BSFC$	Brake specific fuel consumption (g/kWh)
$BSFC_{corr}$	Corrected brake specific fuel consumption (g/kWh)
$BSEC$	Brake specific energy consumption (kJ/kWh)
$BSEC_{corr}$	Corrected brake specific energy consumption (kJ/kWh)
E	Mechanical Energy engine output (kWh)
E_D	Mechanical Energy – diesel mode (kWh)
E_G	Mechanical Energy – gas mode (kWh)
E^{HTC}	Mechanical Energy of the HTC (kWh)
F	Fuel flow rate (kg/s)
FC	Fuel Consumption (kg)
FC_D	Fuel Consumption – diesel mode (kg)
FC_G	Fuel Consumption – gas mode (kg)
FC_{Gd}	Pilot Fuel Consumption – gas mode (kg)
FC^{HTC}	Fuel Consumption with HTC (kg)
J	Mass moment of inertia (kgm^2)
LHV	Lower Heating Value (kJ/kg)
m_{fj}	Burned fuel type j (kg)
P_b	Engine Brake Power (kW)
P_s	Electric Generator Shaft Power (kW)
$\dot{Q}_b$	Combustion heat release rate (kW)
Q_c	Compressor Torque (Nm)
Q_{EM}	Motor/generator Torque (Nm)
Q_l	Friction Torque due to losses (Nm)
Q_t	Turbine Torque (Nm)
SCO_2	Specific CO_2 emission (g/kWh)
SCO_{2corr}	Corrected Specific CO_2 Emission (g/kWh)
SNOx	specific NO_x emission (g/kWh)
$SNOx_{corr}$	Corrected Specific NO_x Emission (g/kWh)
t_d t_G	Operating time intervals (h)
x_b	Cumulative fuel burned fraction (–)
$\dot{x}_b$	Fuel burning rate (s^{-1})
β	Compressor pressure ratio (–)
$\Delta\theta$	Combustion duration (deg)
η_{TC}	Turbocharger efficiency (–)
θ	Engine crank angle (deg)
θ_{SCi}	Start of combustion (deg)
ω_{ij}	EM angular velocity (rad/s)

and 5–15% related to the use of LNG and propulsion plant improvements, respectively. The carbon emissions reduction related to control strategies for the ship propulsion plant was estimated to 3–5% according to [8,9]. A turbo- compound system performance whilst considering its retrofitting on existing engines was investigated in [10], where it is reported that an electrical power output of about 5% of the engine output can be generated, associated with a similar CO_2 emissions reduction.

According to Altosole et al. [11], the Hybrid Turbocharger (HTC) constitutes an attractive solution for improving the efficiency of the ship power plants, contributing towards CO_2 emissions reduction. The HTC system includes an Electric Machinery (EM), which can operate either as a motor or a generator and is connected with the Turbocharger (TC) shaft. In cases where the engine TC operates with a surplus power, this EM operates as generator producing electric power, which can be used to partially cover the ship electric power demand. On the contrary, in cases where a power deficit is anticipated in the engine TC shaft (engine operation at very low loads or fast engine acceleration), the EM operates as a motor providing mechanical power to the TC shaft [12].

The installation of hybrid turbocharging systems leads to the increase of the ship power plant efficiency as well as the ship fuel savings, which are also associated with the reduction of the gaseous emissions. Furthermore, the HTC assists on mitigating or attenuating the TC lag effects [13] as well as substituting the electric driven auxiliary blower used in marine two-stroke engines. However, the HTC installation is associated with an additional cost and it increases the system complexity as well as the involved interactions between the engine and the HTC components.

For adopting new technologies, detailed studies are required to realistically assess the associated benefits and limitations. Several performance, emissions and cost indicators need to be quantified, including efficiency, emissions reduction, technical characteristics such as volume and weight, cost-effectiveness, reliability and maintenance requirements. In addition, the influence of the system on the ship power plant and its behaviour across the whole operating envelope need to be evaluated [14]. To the best of the authors' knowledge, systematic studies focusing on assessing the techno-economic benefits from the use of HTCs in maritime applications are not available.

However, considering the performance of several existing systems as well as the findings of a number of pertinent studies, it can be deduced that the subject is worth for further investigation.

The automotive sector already benefits from the use of HTCs to improve the performance of Diesel Engines (DE), as reported in [15]. One of the first studies focusing on the electrically assisted TC is presented in [16], where a zero dimensional model was employed to simulate the steady state and transient operation of an automotive turbocharged diesel engine.

Nonetheless, due to the challenges of increasing the power plant complexity as well as the additional electric and electronic equipment required for the shipboard HTC use, only limited maritime applications have been reported in the pertinent literature. Furthermore, the HTC technology attracted limited interest from researchers as demonstrated by the very few published studies.

Heim [17] reported the design and testing of a HTC prototype system for increasing the ship power plant efficiency, concluding that the turbocharger efficiency requirements for large two-stroke engines at low loads can be addressed, whilst utilising the surplus energy for electricity generation at high loads.

Ono et al. [18] reported the development and full-scale testing of one of the first HTC consisting of a high speed electric machinery (Motor/Generator) connected to the TC shaft of a large marine low-speed engine (used as the prime mover of a bulk carrier). The EM was interconnected with the ship electric grid by installing an appropriate conversion system. The system trials demonstrated that the generated electric power was in the range 3–4% of the engine power output. The HTC partially covered the ship electric power demand (in parallel with the ship diesel generator sets) at engine loads greater than 60% and fully covered the ship electric energy requirements at engine loads greater than 75%, concluding that this system can operate efficiently for engine loads beyond 60%.

Yang et al. [19] investigated the matching of HTCs with a two-stroke low speed marine engine by using simulation in the GT-Power software, estimating the optimal HTC power values corresponding to the highest engine efficiency at each load, and comparing with the conventional turbocharger. The improvement of the engine Brake Specific Fuel Consumption (BSFC) was found in the range 2–3% depending on the engine operating point.

Nielsen et al. [20] computationally investigated the adoption of the HTC in combination with a selective catalytic reduction system for reducing the NO_x emissions, whilst mitigating the decrease of the engine brake specific fuel consumption. As the NO_x emissions reduction from marine engines represents a long lasting challenge in the shipping industry [21] and [22], the use of HTCs in conjunction with after-treatment technologies is expected to constitute a potential solution. Altosole et al. [11] computationally investigated the HTC usage and its

influence on the performance of a marine four-stroke DF engine (having nominal power of 12 MW) when operating at the gas mode. The electric power delivered to the ship grid was calculated in the range of 4% of the engine brake power; however, the need to reset several control parameters to exploit this benefit was revealed.

From the preceding literature review, the following research gaps were identified: (a) the HTC system effects on the engine performance and emissions have not systematically investigated; (b) the interactions between the HTC and the engine have not been fully addressed; (c) the DF engines operation with HTC in both gas and diesel operating modes have not been analysed; (d) the analysis of HTC systems for ships power plants whilst considering actual operating profiles have not been studied, and; (e) studies on the HTC electric machinery optimal size selection are worthwhile.

The aim of this study is twofold: (a) to systematically investigate and quantify the effects of the HTC system on the performance and emissions of a large marine four-stroke DF engine for both the diesel and gas operating modes considering the entire engine operating envelope; (b) to select the optimal nominal size of the electric motor/generator (EM) of the HTC for a specific ship considering her typical annual operating profile.

The novelty of this study stems from: (a) the thorough investigation of the HTC technology for maritime applications, in particular for a large marine four-stroke engine that is typically employed for covering the propulsion and electric power demands in several ship types including passenger and cruise ships; (b) the quantification of the HTC effects based on metrics including the overall engine system performance, emissions and cost considering the annual operating profile, and; (c) the determination of the optimal rated power of the HTC electric machinery considering the annual power demand operating profile.

The remaining of this study is organised as follows. Section 2 provides a brief description of the employed methods and modelling approaches; in specific, the research methodology is described in Section 2.1, the DF engine model is described in Section 2.2, whereas the HTC submodel description is provided in Section 2.3. Section 3 describes the investigated engine case study. Section 4 presents and discusses the derived results. Finally, Section 5 summarises the conclusions and main findings of this study, also providing recommendations for future research.

2. Methodology and system modelling

2.1. Methodology

This study employs an existing detailed model of the zero/one-dimensional (0D/1D) type developed in the GT Power software by the authors [23].

This model can sufficiently predict the engine performance and emissions parameters effectively representing the interactions between the engine components at both operating modes (gas and diesel).

The followed methodology consists of two phases, which include the numerical investigation of the investigated engine and the selection of the rated power of the HTC electric machinery. These phases and the steps are listed as follows.

- Phase 1: Model set-up, simulation runs and parametric study
  - Step 1.1: Model set-up: the existing 0D/1D model, was extended to accommodate the sub-model of the HTC components
  - Step 1.2: Parametric runs were carried out for both diesel and gas operating modes, considering a wide range of the HTC EM rated power
  - Step 1.3: Simulation results analysis, and identification of the HTC EM power influence on the engine performance and emissions parameters variations
- Phase 2: Optimal HTC EM rated power selection
  - Step 2.1: Actual engine operating profile identification
  - Step 2.2: Key performance indicators (KPIs) selection, constrains and limitations set up
  - Step 2.3: Calculation of the KPIs for both operating modes and the investigated EM rated power values
  - Step 2.4: Optimal EM selection based on KPIs trade offs and set constraints

2.2. Dual fuel engine model

The commercial software GT-Power [24] is employed for modelling the investigated engine with the HTC. The existing model of a marine DF engine, which is described in detail in [23], was extended to incorporate the HTC submodel. This model combines the thermodynamic modelling of the engine components along with the functional modelling of the engine control system. The model is capable of simulating the engine steady state conditions in both operating modes and sufficiently captures the behaviour of the engine components, the control systems response as well as the engine safety system functions. The model was extensively validated against measured engine performance parameters corresponding to steady state and transient conditions exhibiting sufficient accuracy as it is described in the Section 4.1.

Hence, only a brief description of the engine model is provided herein.

The engine cylinder processes are modelled by using the zero-dimensional approach that employs the energy and mass conservation equations along with the ideal gas equation for the calculation of the cylinders working media temperature, mass, pressure, and mixture composition. An one zone approach is used for modelling the gas exchange and compression processes. A two-zone approach is employed for modelling the combustion and expansion processes, where the zones represent the unburned mixture and the burned gas (introduced after the combustion start), respectively [25]. The cylinder gas to wall heat transfer coefficient is calculated by employing the Woschni equation [26]. The Chen-Flynn friction model [27] is used for calculating the engine friction mean effective pressure. The estimation of the NO_x emissions in both operating modes is based on the extended Zeldovich mechanism described in [28] and [29].

The mass flow rates through the engine intake and exhaust valves are calculated by using the quasi-steady adiabatic flow equation considering the respective profiles (equivalent area versus crank angle) and pressure ratios [28]. The engine crank shaft rotational speed is calculated by employing the angular momentum conservation equation.

The engine inlet and exhaust manifolds are modelled by using an one- dimensional approach that employs the mass, momentum, and the energy conversation equations for the calculation of the pressure, velocity, temperature, and composition of the working media (air or exhaust gas) along the manifolds length [24].

For modelling the combustion at the diesel operating mode, a single Wiebe function model is used to calculate the heat release rate, whilst estimating the ignition delay by using the Sitkey equation [30]. This is a semi-predictive combustion modelling approach, which was selected instead of a more detailed predictive multi-zone model or combination of 0D and CFD combustion models. The latter approaches require extensive experimental data for the model constants calibration, and such data were not available for this study.

For modelling the combustion at the gas operating mode, the triple-Wiebe function [25] model is employed considering that each function represents the following consecutive combustion phases: (a) the pre-mixed combustion of a portion of the pilot fuel; (b) the diffusive combustion of the remaining pilot fuel and the rapid burning of the gaseous fuel, and; (c) the cylinder residuals tail combustion [31]. In this operating mode, the ignition delay is approximated by using the data reported in [32] and [33]. The cumulative fuel fraction is calculated according to the following Eq. [24]:

$$x_b = \sum_{i=1}^{3}\left[FF_i\left(1 - e^{-a\left(\frac{\theta-\theta_{SC,i}}{\Delta\theta_i}\right)^{mi+1}}\right)\right] \quad (1)$$

where the subscript i denotes the Wiebe function; FF denotes the weight of each Wiebe function; a is the Wiebe function parameter (considered 6.9); θ denotes the crank angle, θ_{SC} denotes the start of combustion; $\Delta\theta$ is the combustion duration and m denotes the Wiebe function shape factor. It must be noted that only one Wiebe function ($i = 1$) with weight equal to 1 is used for modelling the combustion at the diesel operating mode.

The heat release rate (HRR) is calculated according to Eq. (2), which employs the fuel burning rate (time derivative of the cumulative fuel burned from Eq. (1)) and the total energy from all the injected fuels:

$$\dot{Q}_b = \dot{x}_b \sum_{j=1}^{3}\left(m_{f,j} * LHV_j\right) \quad (2)$$

where $\dot{x}_b$ denotes the fuel burning rate; j denotes the fuel (main diesel, pilot diesel or natural gas); m_f is the burned fuel amount; LHV denotes the fuel lower heating value.

The combustion model parameters (for both operating modes) were calibrated to match the available experimental engine performance data from the engine trials (maximum in-cylinder pressure and brake specific energy consumption). The developed combustion model utilises a database that stores the controlled parameters of the employed Wiebe functions for each operating mode and engine loads 25%, 50%, 75%, 85% and 100% of the MCR. The controlled parameters are the following: for the diesel mode, the combustion duration and shape parameter (m); for the gas mode, the duration, the shape parameter, and the fraction for each Wiebe function. For the diesel mode, the effect of the air–fuel equivalence ratio on the combustion model parameters (shape and combustion duration) was estimated taking into account the Woschni-Anisits equations [30]. At each operating mode, the combustion model parameters were calculated by interpolation between the stored values in the database. To calculate the combustion model parameters during transients with mode changes (gas to diesel, diesel to gas), the model initially calculates the HRR at each mode and subsequently employs interpolation to calculate the HRR considering the energy fractions of the injected fuels (natural gas and diesel).

This model has been employed in previous authors' studies to optimise the engine settings for increasing the engine efficiency as reported in [23], investigate the transient conditions at both operating modes and load changes [34] as well as optimising the engine settings at the diesel mode with exhaust gas re-circulation (EGR) [35]; in the latter case, the combustion model was extended to incorporate the effect of the EGR rate.

2.3. Hybrid turbocharger model

The HTC is modelled considering its components, namely, the compressor, the turbine, the electric machine (EM), and the turbocharger shaft. The mechanical connections of the turbocharger shaft to the compressor impeller, the turbine wheel, and the electric machine are taken into consideration. In addition, appropriate flow connections of the compressor and turbine with the inlet and exhaust manifolds blocks of the engine model are considered.

In specific, the compressor is connected with the engine ambient (upstream) and the engine air cooler (downstream), whereas the turbine is connected between the exhaust manifold (upstream) and the exhaust pipe (downstream). These connections convey the working medium state parameters (pressure, temperature, and gas composition) to the respective turbocharger component. A waste gate, which bypasses a percentage of the exhaust gas along the turbine, is considered connected to the turbine element. The mass flow rate of the waste gate is calculated as a function of the pressure ratio, the waste gate flow area, and the properties of the gas upstream the waste gate.

Only the steady state operating conditions for the engine and the HTC are investigated in this study, assuming that the HTC electric machinery operates as a generator absorbing mechanical power from the turbocharger shaft to generate electric power. The EM mechanical power is calculated by considering the EM shaft torque and rotational speed along with an appropriate mechanical efficiency. The EM electric losses and electric transients were considered out of the scope of this study.

The compressor and turbine are modelled by using their steady state maps, respectively. For the compressor, the following compressor parameters are provided as input in a digitised form: corrected turbocharger shaft speed, pressure ratio, corrected mass flow rate, and isentropic efficiency. For the turbine, the digitised forms of the corrected mass flow rate versus pressure ratio and the efficiency versus pressure ratio are employed. In addition, the reference pressure and temperature are provided as input in both the compressor and turbine. For both the compressor and turbine, the mass flow rate and efficiency are calculated for each computational step by using the respective pressure ratios and the turbocharger shaft speed. Subsequently, the compressor and turbine mechanical powers (absorbed by the compressor impeller/delivered by the turbine wheel) are calculated by employing the energy conservation principle considering the compressor and turbine as open thermodynamic systems.

The HTC shaft angular velocity is calculated by employing Eq. (3), which was derived by considering the HTC shaft angular momentum equilibrium.

$$J\frac{d\omega_m}{dt} = (Q_t - Q_c - Q_{EM} - Q_l) \quad (3)$$

where Q_t [Nm] is the delivered turbine torque, Q_c [Nm] is the absorbed compressor torque, Q_{EM} [Nm] is the EM torque (positive when the EM operates as a generator), Q_l [Nm] denotes the torque lost due to turbocharger shaft mechanical losses, J is the HTC shaft inertia (including the compressor, turbine, EM and shaft inertia) and ω_m is the HTC shaft angular velocity. It must be noted that for the cases where the EM is decoupled, Eq. (3) is also employed to calculate the TC shaft angular velocity (and subsequently the TC shaft rotational speed) by neglecting Q_{EM}.

The torque absorbed by the EM of the HTC is calculated by employing Eq. (4).

$$Q_{EMij} = \frac{1000P_s}{\omega_{ij}} \quad (4)$$

where Ps is the required EM power output (in kW), which was provided as a constant input parameter for in each simulation run, ω is the EM shaft angular velocity (in rad/s), the index i represents the engine operating point (load) and j denotes the engine operating mode (gas or diesel).

2.4. Employed key performance indicators

This study employs several KPIs to quantify the HTC influence on the engine performance and allow for comparing the investigated solutions (engine equipped with and without the HTC).

The first employed KPI is the corrected brake specific fuel consumption, which is defined as the engine brake specific fuel consumption (BSFC) corrected by considering the HTC generated mechanical power, calculated according to Eq. (5).

$$BSFC_{corr} = BSFC\frac{P_b}{P_b + P_s} \quad (5)$$

where P_s represents the HTC electric generator shaft power output (in kW). The measurement of P_s is rather challenging in actual systems, where its estimation is expected based on the measured electrical power and the estimated electric generator efficiency. The engine BSFC (in g/

kWh) is defined according to the following equation:

$$BSFC = 3.6{\cdot}10^{6}\frac{F}{P_b} \tag{6}$$

where F represents the burned fuel mass flow rate (in kg/s) to obtain the engine brake power P_b (in kW). The actual engine BSFC is calculated based on measured data and is corrected according to the process described in ISO3046.

The second employed KPI is the Corrected Brake Specific Energy Consumption defined according to the following equation:

$$BSEC_{corr} = 3600\frac{\sum_j\left(F_j{*}LHV_j\right)}{(P_b + P_s)} \tag{7}$$

where F_j and LHV_j represents the fuel mass flow rate (in kg/s) and the lower heating value (in kJ/kg) of the j^{th} fuel.

To quantify the HTC influence on the engine emissions, the corrected specific NO_x and CO_2 emissions are employed as KPIs, which are calculated by using Eqs. (8) and (9), respectively.

$$SNOx_{corr} = SNOx\frac{P_b}{P_b + P_s} \tag{8}$$

$$\mathrm{SCO_{2corr}} = \mathrm{SCO_2}\frac{P_b}{P_b + P_s} \tag{9}$$

where SNOx and SCO_2 represent the specific emission factors (in g/kWh) for the NOx and CO_2 emissions calculated by the GT-Power model.

The TC efficiency is evaluated by employing the formulation proposed by CIMAC [36], as the ratio between the compression isentropic enthalpy difference (compressor) and the expansion isentropic enthalpy difference (turbine).

The preceding KPIs are calculated for each simulated condition, considering the engine equipped with and without HTC, operating in the diesel and gas mode scenarios. The outcomes of those simulation scenarios are used for the optimal selection of the HTC EM rated size, as presented in Section 4.3.

The KPIs used to quantify the HTC impact on the ship operations is the HTC annual mechanical energy production, the calculation of which requires the definition of the engine operational profile (relationship between load and operating time) as discussed in Section 3. As this study considers that the load profile is based on the engine brake power, an increase of the produced mechanical energy (E) is anticipated for the case of the engine equipped with the HTC in both diesel (E_D) and gas (E_G) modes. This surplus energy is expected to reduce by almost the same amount (affected by the respective losses of the involved electrical system components) the required energy production of the other ship energy producers (generator sets). The evaluation of the energy produced by HTC includes the efficiency of the EM.

The surplus energy available at the diesel (ΔE_D) and gas modes (ΔE_G) is calculated according to the following equation:

$$\Delta E_D = {E_D}^{HTC} - E_D \tag{10}$$

$$\Delta E_G = {E_G}^{HTC} - E_G \tag{11}$$

At each operating point of the load profile, the fuel consumption ($FC_{j,i}$) with and without HTC for both the diesel ($j = D$) and gas ($j = G$) modes is calculated by considering the product of the respective $BSFC$ and the produced engine brake power. The annual fuel consumption for each operating mode (diesel or gas) is calculated by summing up the fuel consumption at each operating point. For the case of the engine without HTC, which is considered the baseline configuration, the annual fuel consumption is evaluated by employing the following equations:

$$FC_D = \sum_i (F_{d,i}t_{d,i}) \tag{12}$$

$$FC_G = \sum_i (F_{G,it}t_{G,i}) \tag{13}$$

$$FC_{Gd} = \sum (F_{Gd,i}\ t_{G,i}) \tag{14}$$

where FCD represents the diesel fuel consumption (in kg), FCG represents the gas fuel consumption (in kg), FCG_d denotes the pilot diesel consumption (in kg), $F_{j,i}$ represents the fuel flow rate (in kg/s) for the j^{th} fuel and the i^{th} load, $t_{d,i}$ and $t_{G,i}$ are the operating time intervals (in s) according to the considered load profile.

Similar equations apply for the engine configuration with the HTC. The differences in the fuel consumption between the engine configurations without and with the HTC for each operating mode are calculated by using the following equations:

$$\Delta FC_D = FC_D - {FC_D}^{HTC} \tag{15}$$

$$\Delta FC_G = FC_G - {FC_G}^{HTC} \tag{16}$$

where the suffix HTC denotes the configuration with the hybrid turbocharger. The fuel savings and the surplus energy available with and without the HTC are presented in Section 4.4.

3. Case studies

3.1. Investigated system description

The configuration of the investigated engine and the HTC is schematically presented in Fig. 1. The EM is mounted on the turbocharger shaft to generate electric power, whereas a frequency converter and a transformer are used for adjusting the generated electric power characteristics (frequency, voltage) of the ship electric network.

The investigated engine is a four-stroke, non-reversible, turbocharged and intercooled DF engine with nine cylinders connected inline. This engine type is typically employed for propulsion and electric power generation in maritime applications. The main engine characteristics are reported in Table 1.

This engine can operate in the gas mode using natural gas as the main fuel and light fuel oil as the pilot fuel; the latter is employed to initiate the combustion. Light or heavy diesel oil can be used as the main fuel in the diesel operating mode. A detailed description of the engine is provided in the engine manufacturer project guide [37].

3.2. Input parameters and assumptions

The following parametric investigations were performed by simulation: (a) for the diesel mode, ten different EM power values in the range 100–1000 kW were considered for the operating points with 25%, 50%, 75%, 85% and 100% loads; (b) for the gas mode, nine values in the range 100–850 kW were considered in the same load range.

This study considers EM of the direct drive permanent magnet type with Insulated Gate Bipolar Transistor (IGBT) power drive. This technology was tested in [38] for medium size, marine two-stroke, diesel engines and is currently adopted in ten shipboard installations with proven records [39]. The power range of the EM selected for the simulations (100–1000 kW) is compatible with the commercially available ranges for permanent magnet motors and the required power electronics. In addition, the power density and dimensions of the permanent magnet EM are, in principle, compatible with the power output expected for HTC turbocharger in large four-stroke engines.

For the energy evaluation, the HTC efficiency is taken as reported in Table 2, which represents the mean values of respective shipboard measurements from [39]. It is also assumed that the efficiency does not depend on the HTC size. This assumption is consistent with the rationale of the present work, which does not address the design of the HTC electrical systems/components, and rather focuses on the HTC impact

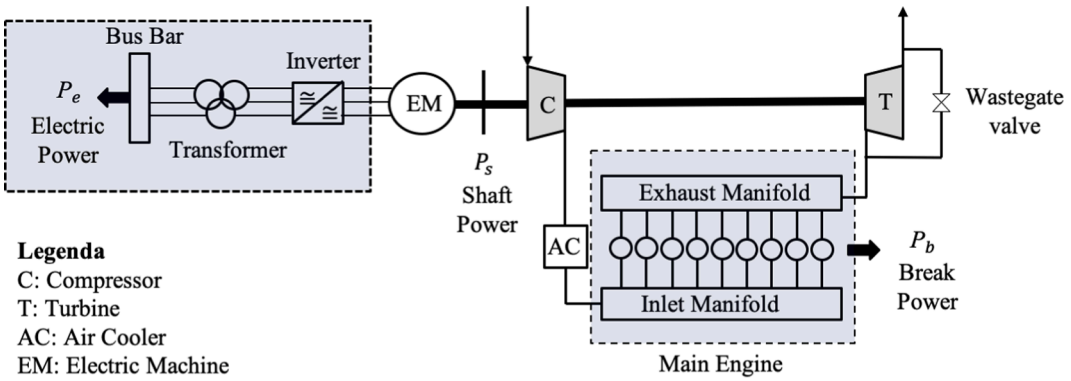

Fig. 1. Schematic of the investigated engine layout with the Hybrid Turbocharger.

Table 1
Main Engine Characteristics adapted from [37].

Engine Characteristics	Unit	Value
Model	–	9L50DF
Power output at MCR[a]	[kW]	8775
Cylinder number	–	9
Engine speed	[rpm]	514
BMEP[b] at MCR	[bar]	20
Bore	[mm]	500
Stroke	[mm]	580
BSEC[c] diesel mode	[kJ/kWh]	8198
BSEC gas mode	[kJ/kWh]	7390
IMO compliance	–	TIER II (diesel mode)
IMO compliance	–	TIER III (gas mode)

[a] Maximum Continuous Rating.
[b] Brake Mean Effective Pressure.
[c] Brake Specific Energy Consumption.

Table 2
HTC electric generator efficiency.

EM load [%]	Efficiency [%]
20	0.86
50	0.92
100	0.94

quantification for shipboard installations.

The engine model set-up requires the following input parameters: (a) geometric data of the engine components; (b) steady state TC components maps; (c) constants for the employed models (stored in the developed database for the combustion model, friction, heat transfer); (d) rated power of the EM; (e) initial conditions for all the parameters for which differential equations are used (e.g., pressure, temperature, speed).

To quantify the advantages of the HTC in terms of ship energy efficiency and exhaust gas emissions, the annual engine load profile reported in [40] for the case of a passenger ship was considered. This profile is provided in Table 3, where the engine load percentage with respect to the power of the Maximum Continuous Rating (MCR) point is reported in the left column, the annual time spent in each load condition is reported in the middle column, and the operating time percentage at each load is provided in the right column. This engine operating profile was derived by considering the following assumptions: (i) the engine is part of a ship power plant consisting of four generator sets; (ii) two or three of these sets (out of four) simultaneously operate, which implies that each engine operates for approximately 44% of the annual ship operating time, and; (iii) the ship annual operating time is equal to 7884 h. To compare the behaviour of the engine with and without HTC, the same load profile was assumed for the two engine operating modes (diesel and gas).

Table 3
Engine load annual profile adapted from [40].

Engine Load	Time	
[% of the MCR power]	[h]	[%]
0.05	16.2	0.21
0.15	124.0	1.57
0.25	215.0	2.73
0.35	1088.5	13.81
0.40	724.0	9.18
0.50	257.3	3.26
0.60	439.7	5.58
0.70	401.1	5.09
0.80	185.9	2.36
0.85	25.0	0.32

3.3. Engine performance parameters limitations

To maintain the engine normal operating conditions and guarantee operation at high turbocharger and engine efficiency ranges, restrictions must be imposed on the generated HTC power. In fact, by increasing the generator power, some engine parameters vary beyond their allowed limits. The recommended values to prevent misfiring and knocking when the engine operates at the gas mode are based on [41], whilst the recommended turbocharger efficiency lower limit was derived from [36]. Other performance parameters recommended ranges/limits were derived based on authors' previous experience and the pertinent literature (e.g., [23,34]). Table 4 reports the restrictions considered in this study for the following parameters: (i) cylinder maximum pressure; (ii) exhaust gas temperature before turbine; (iii) air–fuel equivalence ratio (λ); (iv) turbocharger efficiency. The limitation of the maximum turbocharger shaft speed was also taken into account, however, as this study only considered the case of the HTC generating electric power

Table 4
Recommended engine operating parameters limits.

Parameter	Unit	Limit type	Mode	
			Diesel	Gas
Cylinder maximum pressure	[bar]	upper limit	170	170
Exhaust gas temperature before turbine	[K]	upper limit	893	893
Turbocharger efficiency	[%]	lower limit	60	60
Air–Fuel equivalence ratio	[–]	lower limit	1.8	1.9–2.2
		upper limit		(100% load)

(and not used as motor), this limitation was never exceeded (the TC speed was always lower than the respective one of the baseline case without the HTC).

4. Results and discussion

This section presents the validation of the developed model, the derived model results for a range of HTC EM shaft mechanical power and the calculated KPIs as well as the fuel savings, environmental parameters and cost estimations based on the considered actual operating profile. The section concludes with the selection of the optimal HT EM rated mechanical power.

4.1. Model validation

The developed model for the engine configuration without the HTC was validated against experimental data corresponding to steady state conditions at both operating modes and several loads from 25% to 100% at constant rotational speed (as the engine is used as a generator set operating at 514 rev/min). Table 5 summarises the obtained relative percentage errors between the predicted parameters and their respective measured values, whereas Fig. 2 presents the simulation results (apart from the bottom plots, all others are presented in a normalised format).

Based on these results, the following remarks can be made. The engine operation at the diesel mode is represented with high accuracy, as the obtained percentage errors lay within the range from –2.3% to 2.7%. The predicted parameters closely follow the trends of their respective measured data as demonstrated by the plots shown in Fig. 2. Hence, it is deduced that the model behaviour is quite acceptable and thus, it can be used with confidence for the simulations presented in the following sections. This outcome is attributed to the detail of the modelling approach and the comprehensive process followed to set up and calibrate the model including the accurate estimation of the engine particulars, the use of the actual compressor and turbine maps as well as the calibration of the single Wiebe function combustion model.

Table 5
Relative percentage errors between the predicted model parameters and their respective measured values for the engine steady state operation at the diesel and gas modes.

Load (%)	100	85	75	50	25
Parameter	Diesel Mode				
BSEC	1.0	0.8	1.4	1.4	1.6
Boost pressure	–0.6	–2.3	–1.8	1.5	–1.9
Inlet manifold temperature	0.1	0.2	0.5	0.8	1
TC speed	1.2	0.6	–0.1	2.1	0.1
Exhaust gas temperature before turbine	1.3	1.4	0.6	–0.8	0.4
Exhaust gas temperature after turbine	2.7	3.1	2.6	0.2	2.4
Max. cylinder pressure	–1.1	–1.2	–0.3	2.7	–0.2
NOx emissions	0.9	–	2.3	2.6	1.2
Parameter	Gas Mode				
BSEC	2.9	3.9	2.8	–0.4	0.1
Boost pressure	0	0	0	0	0
Inlet manifold temperature	0	0	–0.2	0	–1.0
TC speed	1.2	0.5	–0.2	1.2	3.9
EWG opening	–2.2	5.2	2.0	5.9	5.5
Exhaust gas temperature before turbine	4.4	5.3	5.5	6.0	8.4
Exhaust gas temperature after turbine	6.3	7.1	7.2	7.3	9.4
Max. cylinder pressure	–2.9	–2.8	–3.0	–5.3	–4.9

(1) The absolute pressure was used for calculating the percentage error.
(2) Temperature in K was used for calculating the percentage error.
(3) At the gas mode, the boost pressure is adjusted by controlling the (EWG) valve opening; the EWG valve is closed at the diesel mode.
(4) *NOx* emissions were not available for 85% load at the diesel mode and all operating points at the gas mode; the predicted *NOx* emission based on the E2 testing cycle (considering the weighting factors of 0.2, 0.5, 0.15 and 0.15 at 100%, 75%, 50% and 25% loads, respectively) [42] was calculated 1.13 g/kWh, whereas the Tier III limit is 2.58 g/kWh [43].

A more diverse model behaviour is exhibited at the gas operating mode, for which the model adjusts the EWG valve opening (via a PI controller) to set the engine boost pressure at a predetermined level (depending on the engine load). This justifies the exhibited relative error in the boost pressure (zero at all loads), which in conjunction with the appropriate modelling of the turbocharging system and the engine air cooler resulted in high accuracy on the prediction of the inlet manifold temperature and the TC speed (with the exception of 25% load where higher –however reasonable– values of the relative errors are exhibited).

As the measured pressure diagrams were not available, to calibrate the combustion model (of the triple Wiebe function type), optimisation was employed at each load with the objective to obtain the minimum weighted error considering the measured values of the in-cylinder maximum pressure and the brake specific energy consumption. This resulted in moderate errors in these two parameters (BSEC and maximum pressure); BSEC exhibited errors in the range from –0.4 to 3.9%, whereas the cylinder maximum pressure values were under-predicted by –5.7% to –2.8%. However, the combustion model inaccuracies (in conjunction with some uncertainty in the measured data) resulted in relatively considerable errors in the prediction of the exhaust gas temperature upstream and downstream the TC turbine (4.4–8.4% and 6.3–9.4%, respectively). Although the model over-predicted the exhaust gas temperature upstream and downstream the turbine, the turbine temperature drop (shown in the bottom-left plot of Fig. 2 was only slightly under-predicted (differences of the measured data and the predicted values were found in the range 5.5–10.5 K; the highest value was exhibited at 25% load).

Based on the preceding discussion, and considering that the predicted parameters for the gas mode follow the trends of their respective measured values (Fig. 2), it is concluded that the developed model can sufficiently represent the investigated marine DF engine steady state operation at both operating modes. It must be noted that this model was also validated for cases with engine operation at transient conditions with mode switching (from diesel to gas and vice versa) as reported in [34]. Hence, the model can be employed with confidence in the investigations presented in the next section.

4.2. Simulation results – HTC impact on the engine performance and emissions parameters

In this section, the results obtained by using the developed model described in Section 2 are presented and discussed. The engine operation at the constant speed of 514 rev/min for both operating modes (diesel and gas) in five different engine loads (specifically, 100%, 85%, 75%, 50%, and 25%

of the engine MCR) is investigated considering several values for the HTC EM shaft mechanical power (P_s) ranging from 0 kW to 1000 kW. It must be noted that the case of 0 kW corresponds to the engine operation without the HTC or the HTC disconnected from its electric generator shaft. A set of the derived simulation results including the turbocharger speed, the engine boost pressure, the exhaust gas temperature before turbine, the air–fuel equivalence ratio, the cylinder maximum pressure, the corrected specific NO_x and CO_2 emissions as well as the Corrected Brake Specific Energy Consumption ($BSEC_{corr}$) are presented in Figs. 3–5. The left plots of these figures present the results for the diesel mode, whereas the right plots provide the results for the gas mode.

For the diesel mode, the exhaust gas waste gate valve is closed for the engine configuration without the HTC (HTC EM mechanical power of 0 kW) and remains closed for the configuration with the HTC operating in any EM shaft mechanical power. The increase of the HTC mechanical power results in the reduction of the TC shaft speed (as the turbine power needs to cover the compressor power, the friction losses and the power delivered to the EM shaft). Thus, the TC over-speed limit is never exceeded as also discussed in Section 3.3. This reduction is gradual for high engine loads (75–100%), whereas more abrupt changes are observed at low loads (25–50%) due to the lower energy content of the

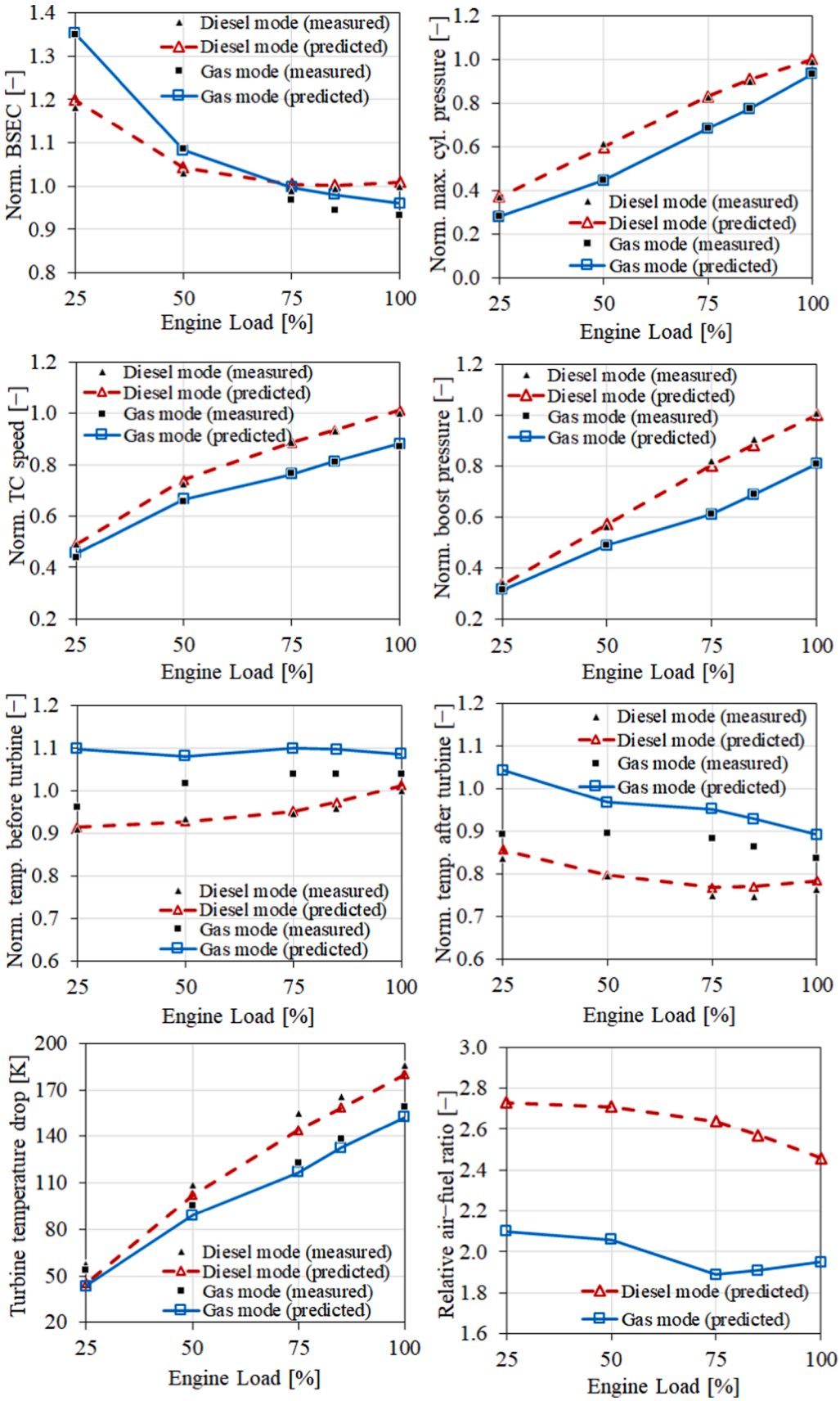

Fig. 2. Simulation results for the engine configuration without the HTC and comparison with the respective experimental data.

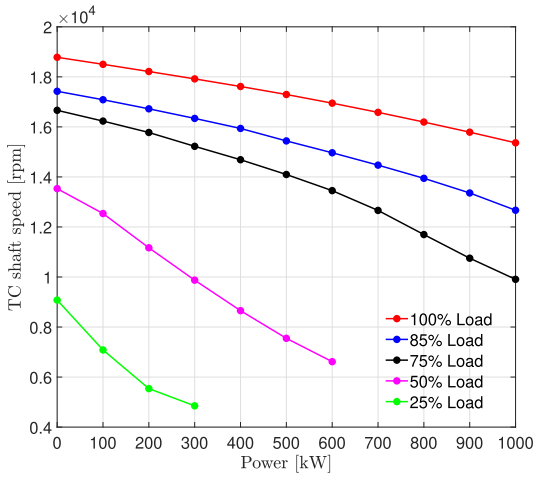

(a) TC shaft speed–Diesel Mode.

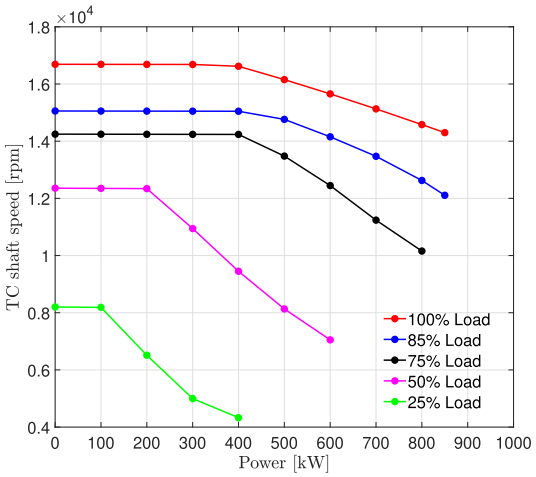

(b) TC shaft speed–Gas Mode.

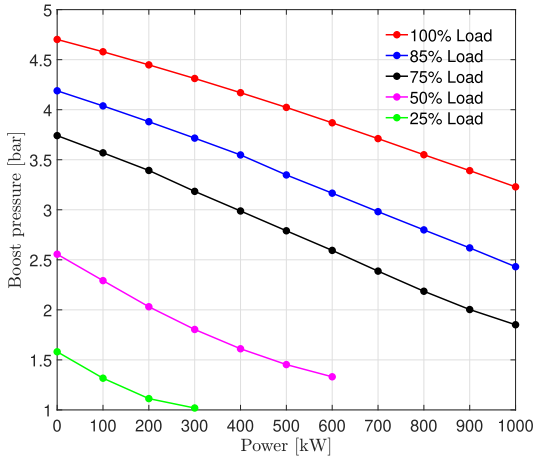

(c) Boost pressure–Diesel Mode.

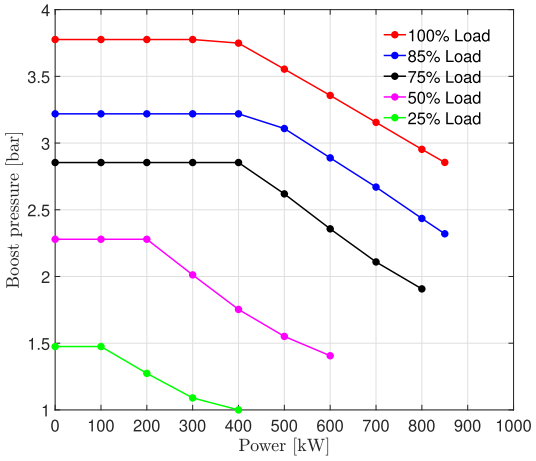

(d) Boost pressure–Gas Mode.

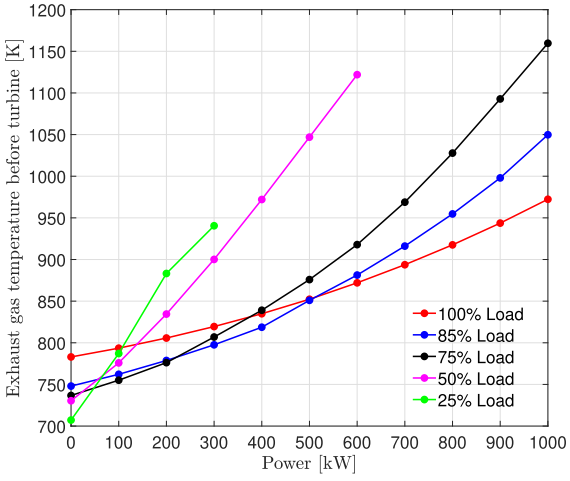

(e) Exhaust gas temperature before turbine–Diesel Mode.

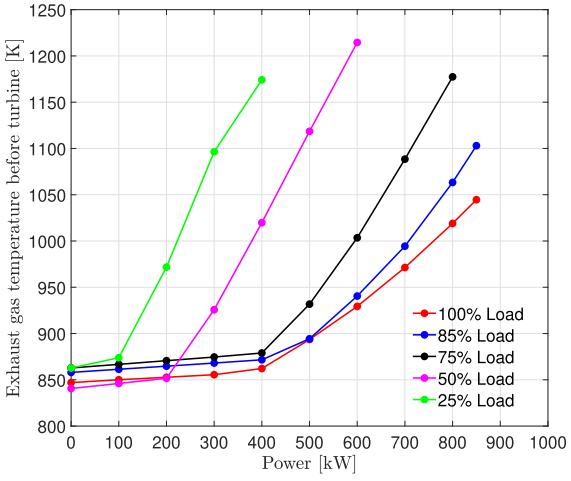

(f) Exhaust gas temperature before turbine–Gas Mode.

Fig. 3. Simulation results – Calculated engine performance parameters versus HTC shaft mechanical power for various engine loads at the diesel and gas operating modes.

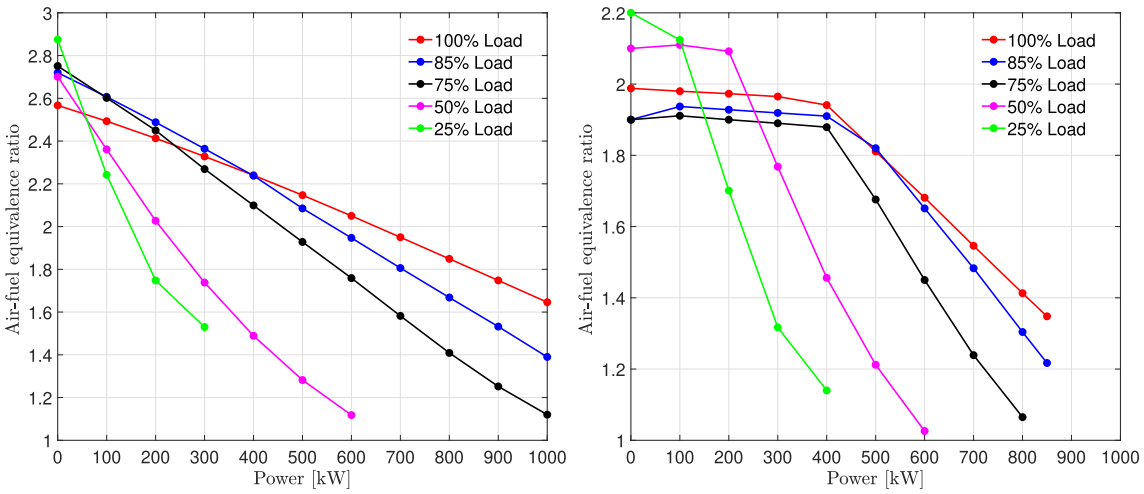

(a) Air–Fuel equivalence ratio–Diesel Mode. (b) Air–Fuel equivalence ratio–Gas Mode.

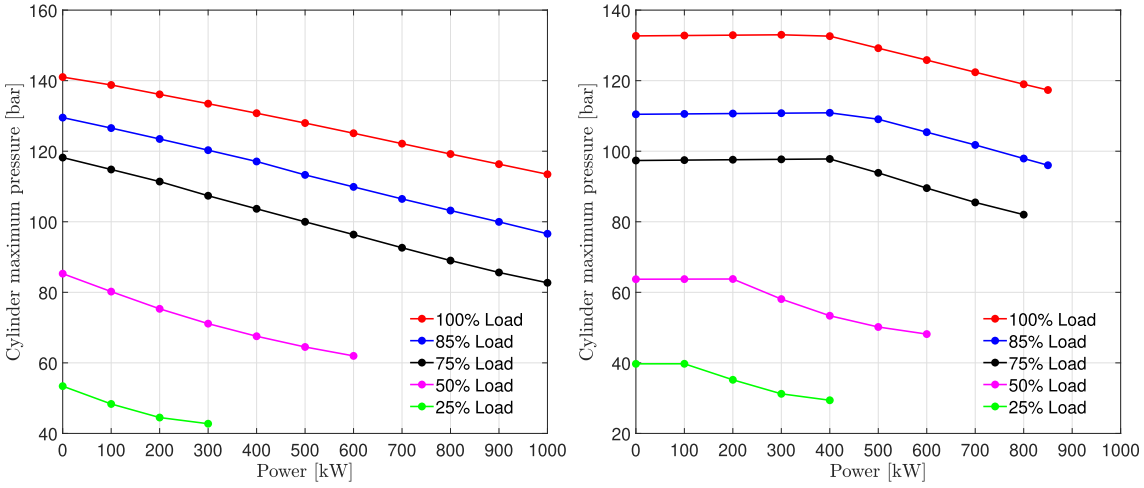

(c) Maximum Cylinder Pressure–Diesel Mode. (d) Maximum Cylinder Pressure–Gas Mode.

Fig. 4. Simulation results – Calculated engine performance parameters versus HTC shaft mechanical power for various engine loads at the diesel and gas operating modes.

gas entering the turbine and the lower TC efficiency. The reduction of the TC shaft speed causes a respective reduction in the engine boost pressure, which results in lower air trapped in the engine cylinders, corresponding to lower air–fuel equivalence ratio. As the fuel amount injected into the engine cylinders varies only slightly (in order for the engine to retain its brake power output), the combustion at lower lambda results in higher exhaust gas temperature values (denoting a resultant increase of the engine thermal loading). Due to the lower boost pressure, the compression and maximum cylinder pressure values reduce.

Taking into account the limits provided in Table 4, the exhaust gas temperature upper limit (893 K) confines the maximum HTC shaft mechanical power in the range of 500–650 kW at the high loads area (75–100%), whereas a maximum mechanical shaft power of 200–290 kW can be delivered in the low loads range. The air–fuel equivalence ratio lower limit (1.8), which allows for the smokeless engine operation, provides the same range for the HTC EM shaft mechanical power at low loads, and slightly higher range (580–850 kW) at high loads. The turbocharger efficiency limitation is discussed in the following section along with the selection of the HTC rated power.

The variations of the corrected brake NO_x emissions shown in Fig. 5 (a) greatly depend on the engine load and the produced HTC EM shaft mechanical power. For the engine operation at high loads (75–100%), with increasing EM shaft power, the corrected brake NO_x slightly increases until the HTC shaft mechanical power reaching a specific value, after which a more abrupt increase is exhibited. This is attributed to the fact that the NO_x emissions depend on the in-cylinder temperature and pressure variations. With the engine operation at higher HTC shaft mechanical power resulting in higher temperature and lower available oxygen for combustion (lower air–fuel equivalence ratio), the produced NO_x emissions increase. In the lower load range, the NO_x emissions increase quite abruptly with the HTC EM shaft mechanical power due to the higher in-cylinder temperature levels (indicated by the respective exhaust gas temperature before turbine). It must be noted that the engine (in the configuration without the HTC) complies with the NO_x Tier II limit (which is 10.5 g/kWh for the specific engine [43]). Therefore, Tier II compliance needs to be retained for the configuration with the HTC. Although the Tier limits are calculated based on a weighted cycle, this value can be considered as another limitation for the HTC EM shaft mechanical power. From Fig. 4(a), it can be deduced that the HTC EM

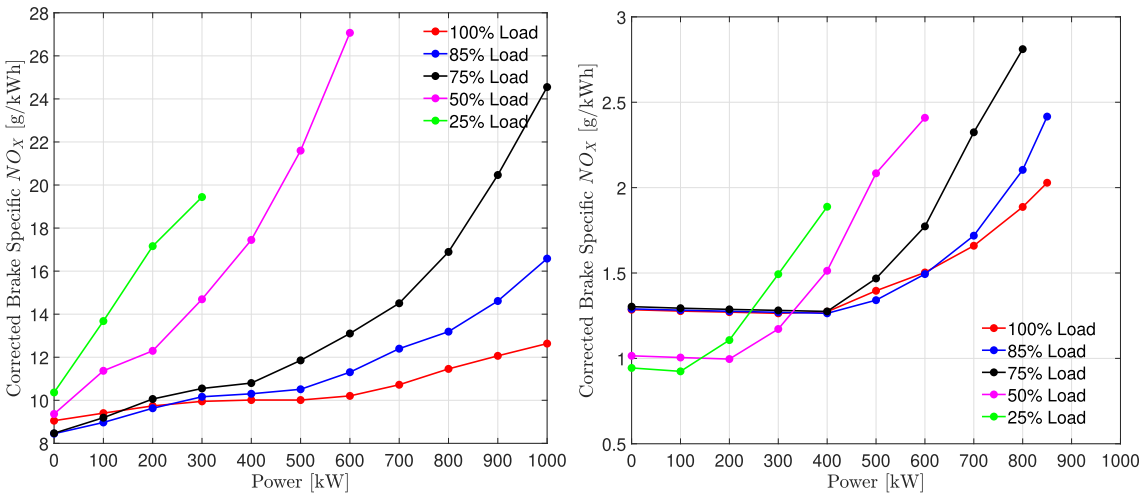

(a) NO_x–Diesel Mode. (b) NO_x–Gas Mode.

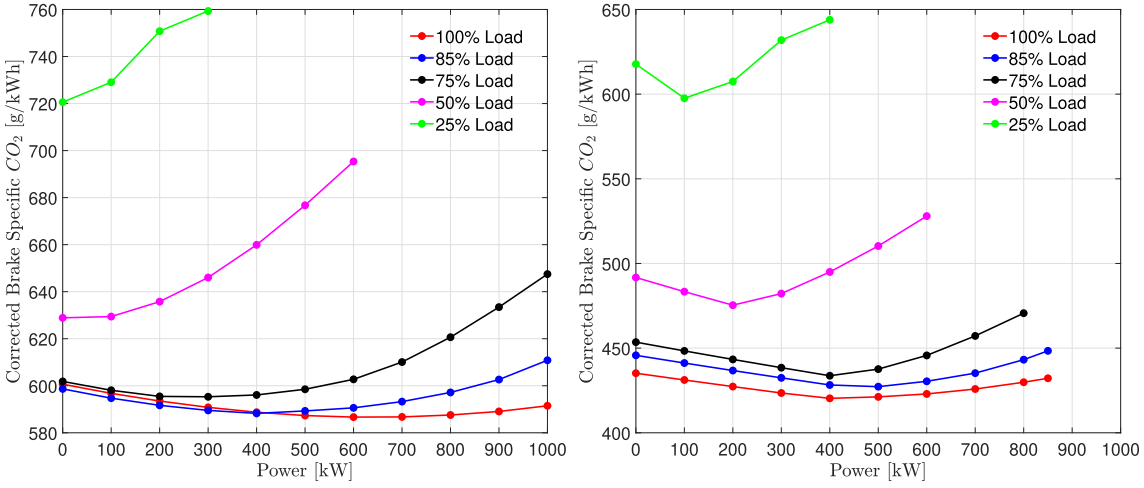

(c) CO_2–Diesel Mode. (d) CO_2–Gas Mode.

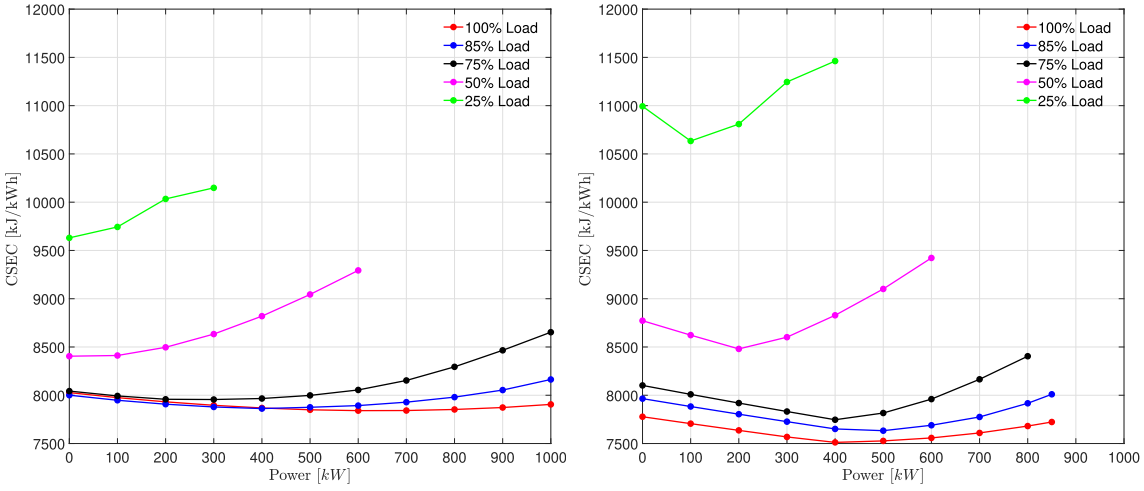

(e) $BSEC_{corr}$–Diesel Mode. (f) $BSEC_{corr}$–Gas Mode.

Fig. 5. Simulation results – Corrected Brake Specific NO_x, CO_2 and $BSEC_{corr}$ versus HTC shaft mechanical power for various engine loads at the diesel and gas operating modes.

shaft power can be around 700 kW for 100% load, and around 300 kW for 75% load. Much lower values for the HTC EM shaft mechanical power can be accepted at low loads.

The derived results for the corrected brake CO_2 emissions, shown in Fig. 5(c), demonstrate that there is an optimal value for the HTC EM shaft mechanical power that minimises this KPI at high loads (75–100%). However, in the case of engine operation at low loads (25% and 50%), the corrected brake CO_2 emissions increase with the HTC EM shaft mechanical power increase, which demonstrates that the operation of the HTC results in a less efficient engine operation.

Similar trends are also observed for the corrected specific energy consumption (calculated according to Eq. (7)), which corresponds to the inverse of the efficiency of the overall engine configuration (including the HTC). These results demonstrate that an optimal range for the HTC EM shaft mechanical power exists that minimises the $BSEC_{corr}$ (maximises the engine efficiency) for the engine operation at high loads. However, the engine operation at low loads results in a higher $BSEC_{corr}$, signifying a lower efficiency for the engine configuration with the HTC.

At the gas mode, the engine (without the HTC) operates by controlling the exhaust gas waste gate (EWG) valve to maintain a predetermined boost pressure at each engine load. The EWG valve remains partially open with its valve area reducing as the load increases [23]. For the engine configuration with the HTC, by increasing the HTC EM shaft mechanical power, the waste gate valve control system responds by closing the EWG valve to retain the set boost pressure, until the point where the EWG valve fully closes. The TC speed also depends on the EWG valve opening and therefore, it exhibits a similar behaviour with the boost pressure, as it is demonstrated from the results presented in Fig. 3. After the point where the EWG valve fully closes, the turbocharger speed, and consequently the boost pressure, considerably reduces with the increase of the HTC shaft mechanical power. The air–fuel equivalence ratio follows the boost pressure response; it almost remains constant for the operating points with constant boost pressure, and then reduces with the increase of the HTC EM shaft mechanical power. As the air–fuel equivalence ratio affects the in-cylinders trapped air, it reflects on the exhaust gas temperature variation, which only slightly increases when the boost pressure remains constant, whereas it considerably increases following the EWG valve closing. The in-cylinder maximum pressure also follows the boost pressure variation trend.

Taking into account the exhaust gas temperature upper limit of 893 K (provided in Table 4), it can be deduced that the engine can withstand a HTC EM shaft mechanical power in the region of 400–500 kW at high loads (75–100%). For the engine operation at low loads, the allowed HTC EM shaft mechanical power is much lower and can reach up to 250 kW for 50% load and 120 kW at 25% load.

The maximum HTC EM shaft mechanical power is also confined by the air–fuel equivalence ratio lower limit (to avoid knocking). At 100% load, the allowed HTC EM shaft power reaches around 450 kW. Values in the region from 200 kW to 300 kW are allowed at low loads (25–50%). The TC efficiency limit is discussed in the next section. According to the engine manufacturer [37], the engine when operating in the gas mode complies with the Tier III NO_x limit, with the NO_x emissions limit being 2.58 g/kWh [43]. Thus, the engine configuration with the HTC must also comply with this limit. As shown in the results of Fig. 5(b), the corrected brake specific NO_x emissions variations initially remain almost constant due to retaining of an almost constant boost pressure (caused by the EWG valve closing) and subsequently considerably increase (after the EWG valve is fully closed). For all the investigated operating points but one (75% and HTC mechanical power of 800 kW), the predicted NO_x emissions were calculated less that the preceding Tier III limit. It must be noted that these results need to be read with some caution, as the employed zero-dimensional two zone model does not provide the exact in-cylinder temperature field, and therefore the predicted NO_x emissions may bear considerable inaccuracies. However, the HTC effect on the NOx emissions variation is clearly depicted in the presented results.

The predicted corrected brake specific CO_2 emissions demonstrate that there is an optimal value for the HTC EM shaft power that minimises this KPI for high engine loads. At low loads, the optimal value (for each load) coincides with the EWG valve closing point, as the corrected brake specific CO_2 emissions increase after this point. Similar trends are observed for the corrected specific energy consumption presented in Fig. 5(f).

4.3. HTC EM shaft mechanical power limitations

The simulation results presented in the previous section demonstrated the engine performance and emissions parameters variations over a wide range of HTC EM shaft mechanical power, and engine loads. The aim of this section is to present the derived metrics and conclude on the optimal HTC size selection.

As reported in [36], the TC efficiency should remain above 0.60 to attain the engine efficiency at high levels. This constraint, along with the other limitations introduced in Table 4 and discussed in the previous section, led to the identification of the maximum HTC EM shaft mechanical power that the engine can withstand at different engine loads, both in the diesel and gas modes. The derived TC efficiency (η_{TC}) against the compressor pressure ratio (β) (which corresponds to engine loads from 25% to 100%) for different values of the HTC EM shaft mechanical power are illustrated in Fig. 6.

The results reported in Fig. 6 demonstrate that the HTC EM maximum shaft power, which the engine can withstand, in the gas mode is lower compared to the respective values in the diesel mode, at all loads. This behaviour, which is aligned with the effects of the other constraints discussed in the previous section (exhaust gas temperature, air–fuel equivalence ratio), is attributed to the reduction of the turbocharger speed, as the HTC EM shaft mechanical power increases, as well as the associated reductions of the compressor and turbine pressure ratios. Similarly to the findings for the previously discussed limitations, the following ranges of the HTC EM shaft power are identified: at the diesel mode, 350–600 kW for high loads (75–100%), 130 kW for 50% load and around 25 kW for 25% load; at the gas mode, 200–450 kW for high loads (75–100%), whereas 100 kW for 50% load and 0 kW (no use of HTC) for 25% load.

The analysis of the corrected brake specific energy consumption $BSEC_{corr}$ and the corrected brake CO_2 emissions, shown in Fig. 5 and discussed in the previous section, demonstrates that the minimum $BSEC_{corr}$ value (and corrected CO_2 value) varies with the engine load, operating mode and the delivered EM shaft mechanical power. For the case of 85% load, a HTC EM shaft mechanical power range of around 400–500 kW provides the minimum $BSEC_{corr}$ value for the gas mode, whereas the respective range is 500–600 kW for the diesel mode.

Tables 6 and 7 present the identified HTC EM maximum power for each limiting factor as well as the minimum corrected CO_2 emissions, for each engine load and operating mode. The identified maximum values of the HTC EM shaft power for each load and operating mode are also illustrated in the last row of these tables. Based on these results, it was deduced that for the investigated marine DF engine, the rated mechanical power of the HTC EM must lie in the range of 100–500 kW. This range is further investigated in the following section. In the case of 25% load, the HTC EM operation results in very low TC efficiency (much lower than the recommended limit of 60%), therefore, it was decided that the HTC EM does not operate in this operating point.

4.4. HTC selection for the considered operating profile

The selection of the optimal EM rated power depends on the fuel consumption and the expected engine power demand profile. Using the operational engine load profile described in Section 3, the annual fuel consumption and the annual produced HTC mechanical energy were calculated considering several values of the HTC EM rated mechanical power. This allows for comparatively assessing the investigated case,

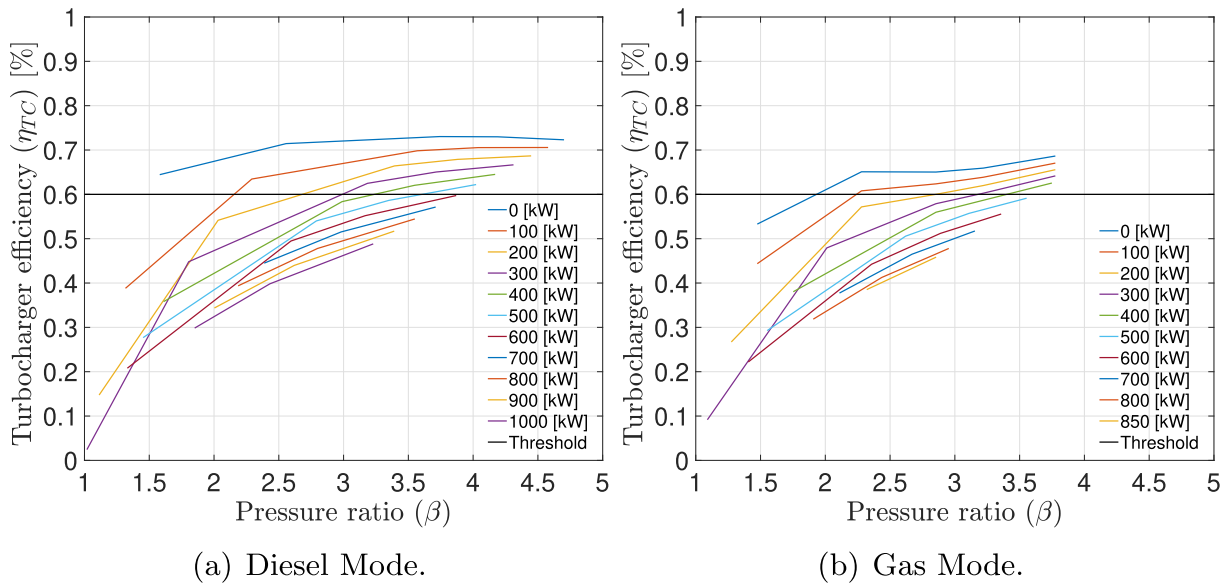

Fig. 6. Turbocharger efficiency versus compressor pressure ratio for various HTC EM shaft mechanical power values.

Table 6
HTC EM maximum mechanical power output considering the set limitations at the Diesel Mode.

Engine Load (%)	100	85	75	50	25
Limiting Parameter	EM power UL [kW]				
Exhaust gas before turbine (UL: 893 K)	680	600	500	280	200
Air–Fuel ratio (LL: 1.8)	750	700	600	500	190
TC efficiency (LL: 0.6)	590	480	360	130	25
NO_x emissions (UL: 10.5 g/kWh)	600	500	300	100	0
CO_2 emissions (minimum)	700	400	300	100	0
HTC EM maximum power	600	400	300	100	0

UL: upper limit; LL: lower limit.

Table 7
HTC EM maximum mechanical power output in kW considering the set limitations at the Gas Mode.

Engine Load (%)	100	85	75	50	25
Limiting Parameter	EM power UL [kW]				
Exhaust gas before turbine (UL: 893 K)	500	500	400	250	100
Air–Fuel ratio (LL:1.9; UL: 2.2)	450	450	400	250	150
TC efficiency (LL: 0.6)	450	300	200	110	0
NO_x emissions (UL: 2.58 g/kWh)	850	850	720	600	400
CO_2 emissions (minimum)	500	500	400	200	100
HTC EM maximum power	500	300	200	100	0

UL: upper limit; LL: lower limit

concluding to the selection of the optimal EM rated power.

In this study, the HTC impact is evaluated in terms of the overall energy delivered by the engine, according to Eqs. (10) and (11), for the diesel and gas operating modes. The overall energy includes the mechanical energy delivered at the engine shaft and the electric energy produced by the HTC and delivered to the ship electrical network.

Table 8 provides the annual surplus energy produced by the engine with the HTC (difference from the energy produced by the engine without the HTC) considering several values for the HTC EM rated mechanical power. The estimated annual surplus energy ranges from 1.7% to 3.0% of the total energy delivered at the engine shaft for the engine configuration without the HTC.

Taking into account the considered engine operating profile, the annual fuel consumption for each operating mode is calculated by Eqs. (12)–(14). The fuel savings compared to the engine configuration without the HTC, which are calculated according to Eqs. (15) and (16), are summarised in Table 9. The fuel savings presented in Table 9 and the annual surplus energy shown in Table 8 represent the overall gain obtained by using the HTC.

Table 8
Annual surplus energy produced by the HTC in the diesel and gas operating modes.

EM	Surplus energy			
Rated Power	Diesel Mode		Gas Mode	
[kW]	[MWh]	[%]	[MWh]	[%]
100	288.5	1.70	288.5	1.70
200	–	–	386.7	2.28
300	484.8	2.86	406.4	2.40
500	504.5	3.0	–	–

Subsequently, the annual fuel cost savings, taking into account both the fuel savings and the surplus energy produced by the HTC, were estimated by considering the three most common marine fuels, namely: Heavy Fuel Oil (HFO), Marine Diesel Oil (MDO), and LNG. The fuels prices used in this study were taken from [44] and other various online sources. The values used in this study are reported in Table 10.

The annual fuel savings as a function of the EM rated mechanical power for the diesel and gas operating modes are illustrated in Fig. 7. These results demonstrate that, for each fuel, there exists a rated power of the By selecting the HTC EM rated mechanical power of 300 kW provides the greatest annual fuel cost savings for the case of the gas operating mode. For the diesel mode, the greatest annual fuel savings

Table 9
Annual fuel mass savings comparing the engine with and without HTC in the diesel and gas operating modes.

EM	Fuel mass savings			
Rated Power	Diesel Mode		Gas Mode	
[kW]	[t]	[%]	[t]	[%]
100	10.30	0.31	40.70	1.37
200	–	–	53.49	1.80
300	21.67	0.66	56.00	1.88
500	22.84	0.69	–	–

Table 10
Fuels prices taken from [44].

Fuel Type	Price [$/t]
Heavy Fuel Oil	300
Marine Diesel Oil	430
Natural Gas	350

HTC EM, which provides the highest annual fuel cost savings.

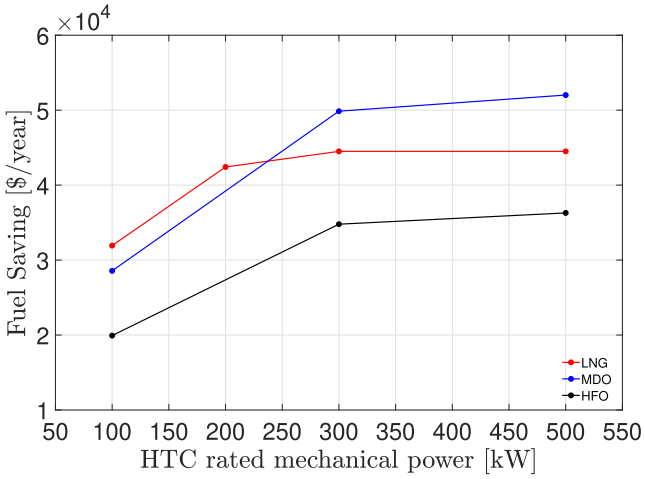

Fig. 7. Annual fuel cost savings as function of the HTC EM rated mechanical power for the diesel and gas operating modes.

are obtained for the EM mechanical rated power of 500 kW.

Considering these findings along with the results for the surplus annual mechanical energy as well as the limitations for the TC efficiency, exhaust gas temperature, and air–fuel ratio presented in the preceding section, it can be deduced that an appropriate selection for the HTC rated mechanical power is 300 kW. This is considered the optimal rated size for the investigated engine operating according to the profile presented in Table 3.

4.5. Comparison of the engine configurations with and without the HTC

In this section, a number of parameters are compared for the cases of the engine configurations with and without the selected HTC (300 kW rated mechanical power for the EM). The original engine configuration (without the HTC) is considered as the baseline configuration in the analysis presented in this section. This comparative assessment aims to highlight the advantages and drawbacks of the engine characteristics in the two engine configurations operating at the diesel and the gas modes.

The TC efficiency for the two engine configurations (with and without the selected HTC) at the diesel and gas modes is presented in Fig. 8(a and b).

At the diesel mode, the TC efficiency for the case of the engine configuration with the selected HTC is greater than the one for the configuration without the HTC for loads above 75% at both operating modes; the TC efficiency difference is around 1% for the 100% load. The opposite occurs for loads lower that 75%; the TC efficiencies difference is 0.8% at 50% load. For the case of 25% load, the same turbocharger efficiency is obtained for the two configurations as the HTC EM is disconnected.

The higher TC efficiency of the configuration with the HTC at high loads at the diesel mode implies that there exists potential for producing additional EM power from the HTC. However, the TC efficiency differences are within 1%, which demonstrates that the selected HTC operating conditions are close to the ones of the baseline configuration.

At the gas mode, the TC efficiencies differences are negligible due to the control of the exhaust gas EWG valve, which results in maintaining the TC speed and the boost pressure in a level comparable to the one of the baseline case. As the obtained TC efficiencies are above the limit of 60% and reach values up to 70–72% at high loads, it can be inferred that the HTC is also effectively matched to the engine and the selection of the 300 kW for the EM rated mechanical power is appropriate.

The engine brake specific fuel consumption (BSFC) for the two engine configurations (with and without the selected HTC) at the diesel and gas mode is presented in Fig. 8(c and d). It can be inferred from these results that the engine BSFC (especially at high loads is slightly improved for the engine configuration with the selected HTC. The corrected BSFC is presented for the engine configuration with the HTC to facilitate the fair comparison of the two configurations. Improvement of around 3 g/kWh was achieved at loads above 75% for the diesel mode, whereas 3–5 g/kWh improvement was obtained at the gas mode. This is attributed to the operating conditions of the engine turbocharging system and the fact that the combustion occurs at slightly lower lambda in comparison with the baseline configuration. In addition, the control of the exhaust gas WG valve to retain an almost constant boost pressure contributes on slightly improving the BSFC at the diesel mode. For the engine configuration with the selected HTC, improvements (reduction) in the BSFC of around 2% at the diesel mode and 3.5–5 g/kWh at the gas mode are achieved.

The break specific NO_x and CO_2 emissions variations versus the engine load for the engine configurations with and without the selected HTC at the diesel and gas modes are presented in Fig. 9. The corrected values of these parameters are presented for the engine configuration with the selected HTC, to facilitate a fair comparison with the respective metrics of the baseline configuration (without the HTC). As it is also discussed in Section 4.2, the engine configuration with the selected HTC exhibits increased NO_x emissions at the diesel mode; however, this engine configuration still complies with the Tier II NO_x limit (10.5 g/kWh for the considered engine). At the gas mode, the engine configuration with the selected HTC exhibits almost the same behaviour (slightly improved though) on the NO_x emissions.

Comparing the respective CO_2 emissions metrics, it can also be inferred that a reduction in the range 2–10 g/kWh is achieved in the configuration with the HTC. Hence, it can be inferred that the HTC contributes on improving the engine environmental footprint in the range 1–3%.

5. Conclusions

This study employed a state-of-the-art model that combines the engine components thermodynamic modelling of the 0D/1D type and the engine control functional modelling. A methodology was followed to investigate via parametric runs the influence of the hybrid turbocharger on the performance and emissions of a large marine dual fuel engine operating at both the diesel and gas modes. Moreover, taking into account an actual operating profile, the HTC electric machinery rated power was selected based on a number of key performance indicators and constrains stemming from the manufacturer limits. This study main findings are summarised as follows.

- The simulation results demonstrated that the engine operation with increasing the HTC power output resulted in lower turbocharger speed, boost pressure, less trapped air and in-cylinder pressure as well as higher exhaust gas temperature.
- The maximum HTC power output is mainly confined by the upper limit in the exhaust gas temperature and the lower limit in the turbocharger efficiency. The corrected specific NO_x emissions were increased providing additional constraints for ensuring the compliance with the IMO NO_x limits. At the engine operation in the gas mode, an additional limitation was introduced from the lower limit of air–fuel ratio to avoid the knocking phenomena.

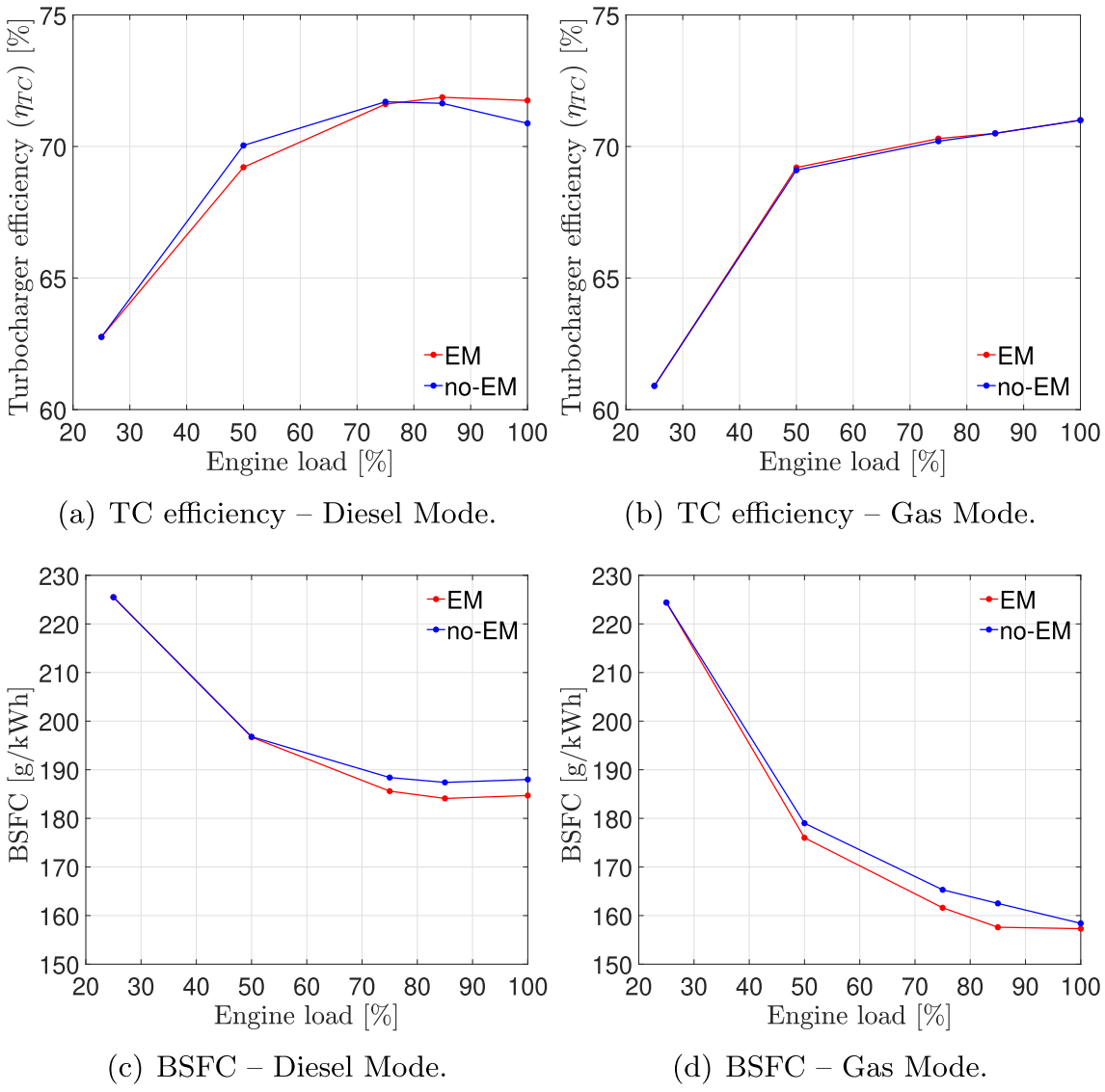

Fig. 8. Performance parameters with and without the selected HTC (300 kW) versus engine load at the diesel and gas operating modes.

- Based on the considered constraints, it was found that the engine configuration with the HTC operating at loads above 50% can provide an additional power output (by the HTC shaft) in the range of 100–500 kW for the diesel mode and up to 400 kW for the gas mode.
- Taking into account a realistic engine operating profile, it was calculated that the HTC annual mechanical energy up to 3% (at the diesel model) and 2.4% (at the gas mode) of the annual engine shaft mechanical energy can be provided. This renders the engine configuration with the HTC attractive for installation on ship power plants.
- Annual savings of the fuel consumption up to 1.9% were predicted for the engine configuration with the HTC (this figure does not include the additional fuel savings associated with the HTC surplus produced power).
- The optimal rated size for the shaft mechanical power of the HTC electric machinery was found to be 300 kW.

The comparison of the performance and emissions parameters of the engine configurations with and without the HTC with the rated mechanical power of 300 kW revealed the following findings.

- The corrected specific fuel consumption and the corrected specific CO_2 emissions were improved by 1–1.5% at the diesel mode and 1–3% at the gas mode for loads above 50%.
- At the diesel mode, the corrected specific NO_X emissions were increased by 15% on average, however the engine remained compliant with the Tier II limit. Improvement of the corrected specific NO_X emissions by 1% was obtained at the gas mode.
- The HTC selected to match the actual engine operating profile can provide an attractive solution for reducing the operational cost and CO_2 emissions of ship power plants.

The novelty of this study stems from the comprehensive investigation and quantification of the HTC impact (benefits, drawbacks) and the engine manufacturer limitations influence in large marine DF four-stroke engines. Those engines are typically used in cruise and passenger ships power plants, thus any small efficiency percentage increase corresponds to considerable environmental and economic benefits. This study provided the tools, framework and comprehensive evidence for achieving a better understanding and thorough insights of the operation of marine dual fuel engines equipped with hybrid turbochargers as well as the underlying parameters that affect the engine performance/emissions and the interactions of the engine subsystems. This study results

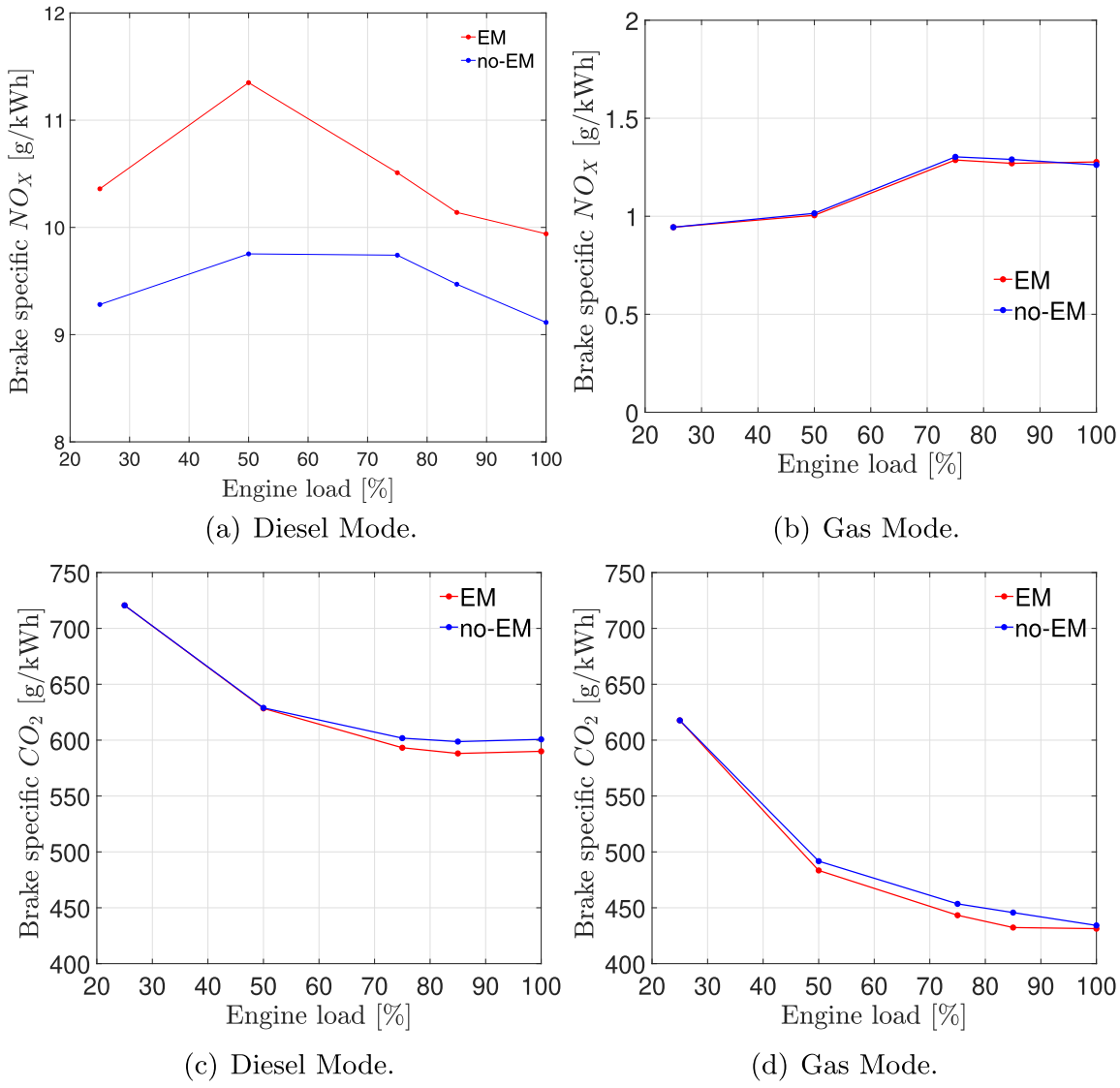

Fig. 9. Corrected Break Specific NO_x and CO_2 emissions for the engine configurations with and without the selected HTC versus engine load at the diesel and gas operating modes.

can be used for providing decision support to the shipping industry to identify and use solutions for decarbonising their operations and reduce operational expenditure. The presented methodology can be customised and applied to other marine engines and power plants categories, thus extending the impact of this study.

Declaration of Competing Interest

The authors declare that they have no known competing financial interests or personal relationships that could have appeared to influence the work reported in this paper.

Acknowledgements

The authors from MSRC greatly acknowledge the funding from DNV AS and RCCL for the MSRC establishment and operation.

The authors gratefully acknowledge that the research presented in this paper was carried out as part of the EU funded H2020 project, VENTuRE (grant no. 856887).

The authors wish to thank Dr. Venky Krishnan, Vice President at Calnetix Technologies, CA, for the provision of valuable data.

The opinions expressed herein are those of the authors and should not be construed to reflect the views of EU, Calnetix, DNV AS and RCCL.

References

[1] R. Zaccone, E. Ottaviani, M. Figari, M. Altosole, Ship voyage optimization for safe and energy-efficient navigation: A dynamic programming approach, Ocean Eng. 153 (2018) 215–224.

[2] H. Wang, W. Mao, L. Eriksson, A three-dimensional dijkstra's algorithm for multi-objective ship voyage optimization, Ocean Eng. 186 (2019) 106–131.

[3] T. Koukaki, A. Tei, Shipping and the environment: How environmental challenges impact on the shipping network, 2020, pp. 330–345.

[4] W. Salmi, J. Vanttola, M. Elg, M. Kuosa, R. Lahdelma, Using waste heat of ship as energy source for an absorption refrigeration system, Appl. Therm. Eng. 115 (1) (2017) 501–516.

[5] L. Wei, P. Geng, A review on natural gas/diesel dual fuel combustion, emissions and performance, Fuel Process. Technol. 142 (2016) 264–278.

[6] International Maritime Organization, Amendments to the annex of the protocol of 1997 to amend the international convention for the prevention of pollution from ships, 1973, as modified by the protocol of 1978 relating thereto, https://www.epa.gov/sites/production/files/2016-09/documents/ resolution-mepc-202-62 -7-15-2011.pdf (2011).

[7] E.A. Bouman, E. Lindstad, A.I. Rialland, A.H. Strømman, State-of- the-art technologies, measures, and potential for reducing ghg emissions from shipping – a review, Transp. Res. Part D: Transp. Environ. 52 (2017) 408–421.

[8] M. Figari, C. Guedes Soares, Fuel consumption and exhaust emissions reduction by dynamic propeller pitch control, in: Proceedings of MARSTRUCT 2009, 2nd International Conference on Marine Structures-Analysis and Design of Marine Structures (2009) 543–550.

[9] S. Michetti, M. Ratto, A. Spadoni, M. Figari, M. Altosole, G. Marcilli, Ship control system wide integration and the use of dynamic simulation techniques in the fremm project, in: International Conference on Electrical Systems for Aircraft, Railway and Ship Propulsion, ESARS 2010.
[10] K. Shiraishi, Y. Ono, Hybrid turbocharger with integrated high speed motor-generator, Technical Review: Mitsubishi Heavy Industries, Ltd 44 (1).
[11] M. Altosole, G. Benvenuto, U. Campora, F. Silvestro, G. Terlizzi, Efficiency improvement of a natural gas marine engine using a hybrid turbocharger, Energies 11 (8) (2018) 1924.
[12] Y. Ono, K. Shiraishi, K. Sakamoto, Y. Ito, Development of new turbocharger technologies for energy efficiency and low emissions, in: 10th International Conference on Turbochargers and Turbocharging, 2012, pp. 365–374.
[13] A.G. Gravdal, Diesel engine response improvements using hybrid turbocharging (2017).
[14] G.J. Tzortzis, C.A. Frangopoulos, Dynamic optimization of synthesis, design and operation of marine energy systems, Proc. Instit. Mech. Engineers, Part M: J. Eng. Maritime Environ. 233 (2) (2019) 454–473.
[15] B. Padhiyar, P.K. Sharma, Application of hybrid turbocharger to improve performance of engine, IJEET 1 (2014) 1–2014.
[16] T. Katrašnik, S. Rodman Opresnik, F. Trenc, A. Hribernik, V. Medica, Improvement of the dynamic characteristic of an automotive engine by a turbocharger assisted by an electric motor, J. Eng. Gas Turb. Power-T ASME 125.
[17] K. Heim, Existing and future demands on the turbocharging of modern large two-stroke diesel engines, in: 8th Supercharging Conference, Dresden, 2002, pp. 1–2.
[18] Y. Ono, K. Shiraishi, Y. Yamashita, Application of a large hybrid turbocharger for marine electric-power generation, Vol. 49, 2012, p. 29.
[19] M. Yang, C. Hu, Y. Bai, K. Deng, Y. Gu, Y. Qian, B. Liu, Matching method of electric turbo compound for two-stroke low-speed marine diesel engine, Appl. Therm. Eng. 158.
[20] J.B. Nielsen, K.K. Yum, E. Pedersen, Improving pre-turbine selective catalytic reduction systems in marine two-stroke diesel engines using hybrid turbocharging: A numerical study of selective catalytic reduction operation range and system fuel efficiency, Proc. Instit. Mech. Engineers, Part M: J. Eng. Maritime Environ. 234 (2) (2020) 463–474.
[21] J. Kowalski, W. Tarelko, Nox emission from a two-stroke ship engine. Part 1: Modeling aspect, Appl. Therm. Eng. 29 (11–12) (2009) 2153–2159.
[22] J. Kowalski, W. Tarelko, NOx emission from a two-stroke ship engine: Part 2 – Laboratory test, Appl. Therm. Eng. 29 (11-12) (2009) 2160–2165.
[23] S. Stoumpos, G. Theotokatos, E. Boulougouris, D. Vassalos, I. Lazakis, G. Livanos, Marine dual fuel engine modelling and parametric investigation of engine settings effect on performance-emissions trade- offs, Ocean Eng. 157 (2018) 376–386.
[24] Gamma Technologies, GT-SUITE manual (2018).
[25] G.P. Merker, C. Schwarz, G. Stiesch, F. Otto, Simulating Combustion, Springer.
[26] G. Woschni, A universally applicable equation for the instantaneous heat transfer coefficient in the internal combustion engine, Tech. rep., SAE Technical paper (1967).
[27] R. Papagiannakis, C. Rakopoulos, D. Hountalas, E. Giakoumis, Study of the performance and exhaust emissions of a spark-ignited engine operating on syngas fuel, Int. J. Altern. Propul. 1 (2/3) (2007) 190–215.
[28] G.A. Lavoie, J.B. Heywood, J.C. Keck, Experimental and theoretical study of nitric oxide formation in internal combustion engines, Combust. Sci. Technol. 1 (4) (1970) 313–326.
[29] S. Salimian, R.K. Hanson, C.H. Kruger, High temperature study of the reactions of o and oh with nh3, Int. J. Chem. Kinet. 16 (6) (1984) 725–739.
[30] G.P. Merker, C. Schwarz, G. Stiesch, F. Otto, Simulating Combustion: Simulation of combustion and pollutant formation for engine-development, Springer Science & Business Media, 2005.
[31] G.A. Karim, Dual-fuel diesel engines, CRC Press, 2015.
[32] E. Sixel, J. Hiltner, C. Rickert, Use of 1-d simulation tools with a physical combustion model for the development of diesel-gas or DF engines. CIMAC Congress, 2016.
[33] C. Christen, D. Brand, Imo tier 3: gas and dual fuel engines as a clean and efficient solution. Proceedings: Conseil International Des Machines A Combustion (CIMAC) Congress, 2013.
[34] S. Stoumpos, G. Theotokatos, C. Mavrelos, E. Boulougouris, Towards marine dual fuel engines digital twins—integrated modelling of thermodynamic processes and control system functions, J. Mar. Sci. Eng. 8(3).
[35] S. Stoumpos, G. Theotokatos, Multiobjective optimisation of a marine dual fuel engine equipped with exhaust gas recirculation and air bypass systems, Energies 13 (19).
[36] The International Council on Combustion Engines, Turbocharging efficiencies – definitions and guidelines for measurement and calculation, https://www.cimac.com/cms/upload/Publication_ Press/Recommendations/Recommendation_27_rev_081007.pdf, online; accessed 29 July 2020 (2007).
[37] Wärtsilä, Wärtsilä 50df product guide, http://cdn.wartsila. com/docs/default-source/product-files/engines/dfengine/product-guide-oe-w50df.pdf (2012).
[38] K. Shiraishi, V. Krishnan, Electro-assist turbo for marine turbocharged diesel engines, in: Proceedings of ASME Turbo Expo 2014: Turbine Technical Conference and Exposition, no. GT2014-25667, 2014.
[39] V. Krishnan, Calnetix technologies, cerritos ca 90703, Private Communications.
[40] F. Baldi, F. Ahlgren, T.-V. Nguyen, M. Thern, K. Andersson, Energy and exergy analysis of a cruise ship, Energies 11 (10) (2018) 2508.
[41] Wärtsilä, Wärtsilä medium-speed engines [cited 20.08.20]. URL https://pdf.nauticexpo.com/pdf/waertsilae-corporation/waertsilae-medium-speed-engines/24872-69921.html.
[42] International Maritime Organization, Appendix ii – test cycles and weighting factors – marpol annex vi regulation 13, http://www.marpoltraining.com/MMSKOREAN/MARPOL/Annex_VI/app2.htm (2008).
[43] International Maritime Organization, Nitrogen oxides (nox) – marpol annex vi regulation 13, https://wwww.imo.org/en/OurWork/ Environment/Pages/Nitrogen-oxides-(NOx)—Regulation-13.aspx (2008).
[44] N.L. Trivyza, A. Rentizelas, G. Theotokatos, A novel multi-objective decision support method for ship energy systems synthesis to enhance sustainability, Energy Convers. Manage. 168 (2018) 128–149.